Synthesis and study of Cu^{II} complex with nitroxide, a jumping crystal analog

R. Z. Sagdeev,[a,b] S. E. Tolstikov,[a] S. V. Fokin,[a] I. V. Obsharova,[a] S. V. Tumanov,[a,c] S. L. Veber,[a,c] G. V. Romanenko,[a] A. S. Bogomyakov,[a] M. V. Fedin,[a,c] E. V. Tretyakov,[d] M. Halcrow,[e] and V. I. Ovcharenko[a]*

[a] *International Tomography Center, Siberian Branch of the Russian Academy of Sciences, 3a ul. Institutskaya, 630090 Novosibirsk, Russian Federation. E-mail: tse@tomo.nsc.ru*
[b] *Kazan (Volga Region) Federal University, 18 ul. Kremlevskaya, 420008 Kazan, Russian Federation*
[c] *Novosibirsk State University, 2 ul. Pirogova, 630090 Novosibirsk, Russian Federation*
[d] *N. N. Vorozhtsov Novosibirsk Institute of Organic Chemistry, Siberian Branch of the Russian Academy of Sciences, 9 prosp. Akad. Lavrent´eva, 630090 Novosibirsk, Russian Federation*
[e] *University of Leeds, United Kingdom, Leeds, LS2 9JT*

We synthesized 1-ethylimidazolyl-substituted nitronyl nitroxides, *i.e.*, 2-(1-ethylimidazol-4-yl)- (L^{4Et}) and 2-(1-ethylimidazol-5-yl)-4,4,5,5-tetramethyl-4,5-dihydro-1*H*-imidazole 3-oxide-1-oxyl (L^{5Et}). The stable radical L^{5Et} is an ethyl analog of 2-(1-methylimidazol-5-yl)-4,4,5,5-tetramethyl-4,5-dihydro-1*H*-imidazole 3-oxide-1-oxyl (L^{5Me}) described earlier, the reaction of which with $Cu(hfac)_2$ (hfac is 1,1,1,5,5,5-hexafluoropentane-2,4-dionate) leads to the formation of the $[Cu(hfac)_2(L^{5Me})_2]$ jumping crystals. The reaction of $Cu(hfac)_2$ with L^{5Et} with reagent ratios 1 : 2 and 1 : 1 yields heterospin complexes $[Cu(hfac)_2(L^{5Et})_2]$ and $[Cu(hfac)_2L^{5Et}]_2$, respectively. X-ray diffraction study of the mononuclear complex $[Cu(hfac)_2(L^{5Et})_2]$ determined that the compound has a packing similar to that of jumping crystals studied earlier, with the only difference being that the O...O contacts between neighboring nitroxide groups were found to be 0.3—0.5 Å longer than in $[Cu(hfac)_2(L^{5Me})_2]$. As a result of the lengthening of these contacts, $[Cu(hfac)_2(L^{5Et})_2]$ crystals lack chemomechanical activity. We found that when cooling crystals of binuclear complex $[Cu(hfac)_2L^{5Et}]_2$ below 50 K, the antiferromagnetic exchange between unpaired electrons of the >N—•O groups of neighboring molecules leads to the full spin-pairing of the nitroxides, with only the Cu^{2+} ions contributing to the residual paramagnetism of the compound.

Key words: Cu^{2+}, nitroxide radicals, X-ray diffraction, magnetic properties.

Recently, transition metal hexafluoroacetylacetonate complexes with a nitronyl nitroxide radical, namely, 2-(1-methylimidazol-5-yl)-4,4,5,5-tetramethyl-4,5-dihydro-1*H*-imidazole 3-oxide-1-oxyl (L^{5Me}), given by the general formula $[M(hfac)_2(L^{5Me})_2]$, where M = Mn^{2+}, Co^{2+}, Ni^{2+}, Cu^{2+}; hfac is 1,1,1,5,5,5-hexafluoropentane-2,4-dionate, were described. A specific feature of the $[M(hfac)_2(L^{5Me})_2]$ crystals is their ability to spontaneously move when excited with heat or light, owing to which they were named jumping.[1] In the solid phase of $[M(hfac)_2(L^{5Me})_2]$, the deoxygenation reaction occurs, during which the starting complex with nitronyl nitroxide transforms into a complex with the corresponding imino nitroxide. These complexes (the complex with nitronyl nitroxide and the complex with imino nitroxide) form limited regions of solid solutions causing an increase of strain in the crystals over the course of a gradually proceeding solid phase reaction and their subsequent destruction.[2,3] In the study of the jumping crystal effect, both the metal-containing matrix and the paramagnetic ligand were modified.[2,3] The crucial role of the heterospin crystal packing in the possibility of the appearance of chemomechanical activity was demonstrated. When varying the transition metal ion in the $M(hfac)_2$ matrix and replacing the methyl substituent in L^{5Me} with a CD_3 group (*i.e.*, going from L^{5Me} to L^{5CD3}), the chemomechanical activity of crystals remained the same. However, the substitution of the imidazole ring with a triazole one, *i.e.*, going from L^{5Me} to the topologically related, in terms of structure, 2-(1-methyl-1,2,3-triazol-5-yl)-4,4,5,5-tetramethyl-2-imidazoline 3-oxide-1-oxyl (L^{Tr}), quenches the chemomechanical activity of the crystals.[2,3]

Published in Russian in *Izvestiya Akademii Nauk. Seriya Khimicheskaya,* No. 2, pp. 0222—0230, February, 2017.
1066-5285/17/6602-0222

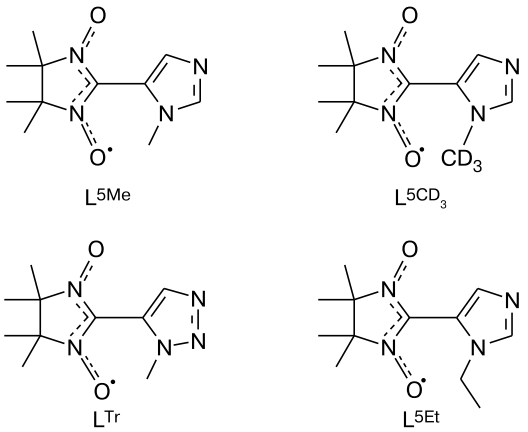

As a continuation of these studies, we synthesized and investigated the structure and properties of the heterospin complex Cu(hfac)$_2$ with L^{5Et}, an ethyl analog of L^{5Me}.

Results and Discussion

The L^{5Et} nitronyl nitroxide was obtained from 1*H*-imidazole-4-carbaldehyde in a similar manner to the synthesis of L^{5Me}.[4] This synthesis produced the target L^{5Et} and its isomer L^{4Et}, with their yields calculated on the starting 1*H*-imidazole-4-carbaldehyde being equal to 8.5 and 5.6%, respectively. Attempted ethylations of a spin-labeled imidazole produced exclusively L^{4Et} (Scheme 1).

The L^{4Et} and L^{5Et} nitronyl nitroxides were successfully grown as single crystals and their molecular and crystal structures were determined. The molecular structures of the radicals are shown in Fig. 1. For the L^{4Et} and L^{5Et} molecules, the bond lengths in the N—O groups are typical of nitroxides and lie in the range of 1.279(2)—1.285(2) Å.[5] The O•—N—C=N→O angle between the planes of the imidazole ring and the nitronyl nitroxide moiety is equal to 13.0° and 39.0° for L^{4Et} and L^{5Et}, respectively, while the angle between the ethyl group (Et—N) and the imidazole ring is 60.5 and 77.2°, respectively.

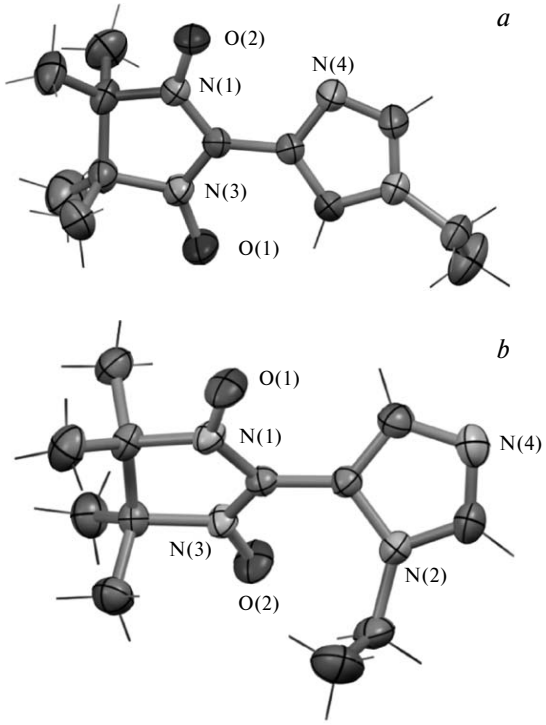

Fig. 1. Molecular structures of L^{4Et} (*a*) and L^{5Et} (*b*). The ellipsoids are drawn at 50% probability.

The temperature dependences of the effective magnetic moment $\mu_{eff}(T)$ for L^{4Et} and L^{5Et} are shown in Fig. 2. For both radicals the μ_{eff} value is 1.73 μ_B at 300 K, which is in good agreement with the theoretical spin-only value for one paramagnetic center with spin $S = 1/2$ ($g = 2$), confirming the high purity of the isolated nitroxides. When decreasing the temperature, the μ_{eff} value for L^{5Et} gradually decreases to 0.09 μ_B at 2 K, while the μ_{eff} value for L^{4Et} is virtually unchanged when decreasing the temperature to 10 K and only then increases slightly to 1.88 μ_B at 2 K. The experimental $\mu_{eff}(T)$ dependences can be adequately described within the framework of the theoretical model of exchange-coupled dimers ($H = -2J \cdot S_1S_2$) with the

Scheme 1

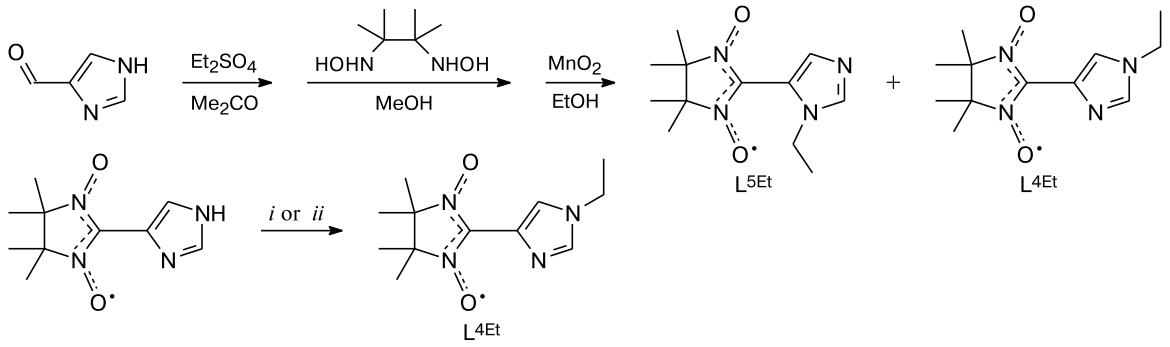

Reaction conditions: *i.* Et_2SO_4/Me_2CO; *ii.* Bu^tOK, then Et_2SO_4/DMF.

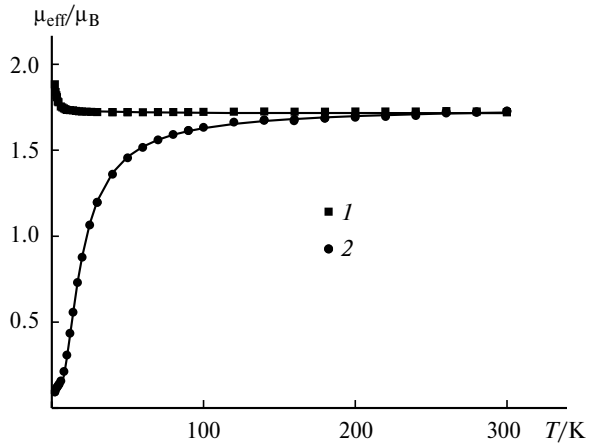

Fig. 2. Temperature dependences of the effective magnetic moment (μ_{eff}) for L^{4Et} (*1*) and L^{5Et} (*2*). The solid lines represent the theoretical curves.

exchange interaction parameters J/k equal to −25.8 and 0.82 K for L^{5Et} and L^{4Et}, respectively (see Fig. 2).

While studying the products of the reaction of $Cu(hfac)_2$ with L^{5Et}, the mononuclear ($[Cu(hfac)_2(L^{5Et})_2]$) and the binuclear ($[Cu(hfac)_2L^{5Et}]_2$) complexes were isolated. The solid phase structure of $[Cu(hfac)_2(L^{5Et})_2]$ is similar to that of $[Cu(hfac)_2(L^{5Me})_2]$ described earlier,[1] with the crystals possessing chemomechanical activity. A favorable factor for the appearance of this property is such a packing of molecules in the $[Cu(hfac)_2(L^{5Me})_2]$ crystal, in which the O_{NO} atoms are grouped in fours with a short central O...O bond length and longer distances between terminal groups and between the fours (Fig. 3, *a*). A similar packing is also present in the $[Cu(hfac)_2(L^{5Et})_2]$ crystals; however, the O...O distance there is considerably longer (see Fig. 3, *b*). This suggests that the long intermolecular distances are responsible for the absence of chemomechanical activity in the $[Cu(hfac)_2(L^{5Et})_2]$ crystals (the samples of complex crystals exhibited mechanical activity neither when irradiated, nor when heated). It should be noted that the differences in the geometry of the $[Cu(hfac)_2(L^{5Me})_2]$ and $[Cu(hfac)_2(L^{5Et})_2]$ molecules themselves are insignificant (Table 1).

A $\mu_{eff}(T)$ plot for $[Cu(hfac)_2(L^{5Et})_2]$ is shown in Fig. 4. At 300 K, μ_{eff} is 3.04 μ_B, when decreasing the temperature to 80 K it remains virtually unchanged, until it decreases to 1.76 μ_B at 2 K. The high-temperature moment value is in good agreement with the theoretical spin-only value for three paramagnetic centers with spins $S = 1/2$ (two nitr-

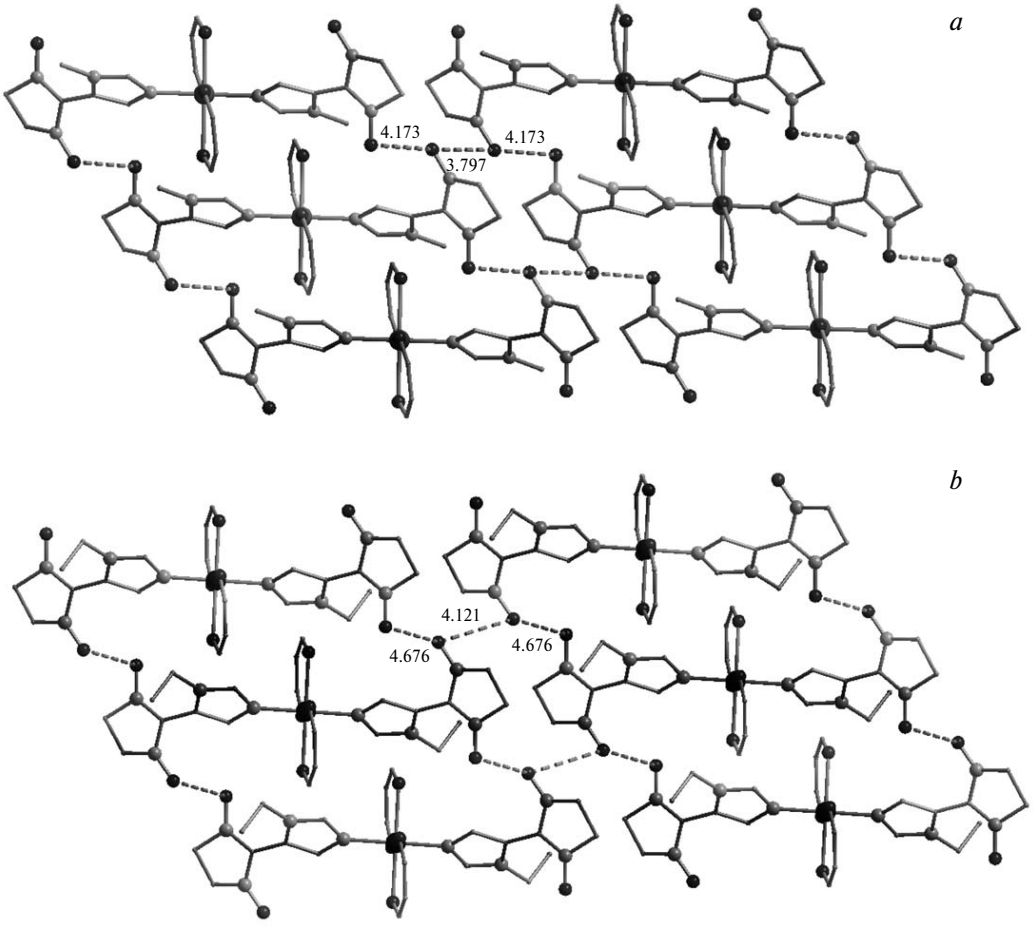

Fig. 3. Molecular packing of $[Cu(hfac)_2(L^{5Me})_2]$ (*a*) and $[Cu(hfac)_2(L^{5Et})_2]$ (*b*).

Table 1. Selected bond lengths and angles in the $[Cu(hfac)_2(L^{5Me})_2]$ and $[Cu(hfac)_2(L^{5Et})_2]$ molecules

Parameter (see Ref. 1)	$[Cu(hfac)_2(L^{5Me})_2]$ 305 K	$[Cu(hfac)_2(L^{5Et})_2]$ 295 K
Bond/Å		
Cu—O	1.995(2), 2.292(3)	1.997(5), 2.262(6)
Cu—N_{Im}	1.998(3)	1.981(6)
N—O	1.278(4), 1.272(4)	1.280(8), 1.253(8)
Angle/deg		
(Et—N)—Im	—	69.2
CN_2—Im	45.8	45.7

oxide radicals and one Cu^{2+} ion). A decrease in μ_{eff} indicates the presence of antiferromagnetic exchange in the solid phase of the complex caused by short contacts between nitroxides of neighboring molecules. In fact, the experimental $\mu_{eff}(T)$ dependence can be adequately described in the approximation of the sum of contributions of the exchange-coupled nitroxides ($H = -2J \cdot S_1S_2$) and the Cu^{2+} ion (see Fig. 4) to magnetic susceptibility. The optimal parameter values are: $g = 2.0$, the exchange interaction parameter $J/k = -9.5$ K, and the Curie constant $C = 0.425$ K cm^3 mol^{-1}. The Curie constant C is in good agreement with the theoretical value of 0.421 K cm^3 mol^{-1} for one Cu^{2+} ion at $g = 2.12$. Since the intramolecular exchange between the Cu^{2+} ion spins and the coordinated radicals is small,[6,7] it was neglected.

The binuclear complex $[Cu(hfac)_2L^{5Et}]_2$ was obtained using the reagent ratio 1 : 1. As a result of bridging coordination of radical molecules, 14-membered metallocycles are formed (Fig. 5).

Table 2 gives selected bond lengths and bond angles in the $[Cu(hfac)_2L^{5Et}]_2$ molecule at different temperatures

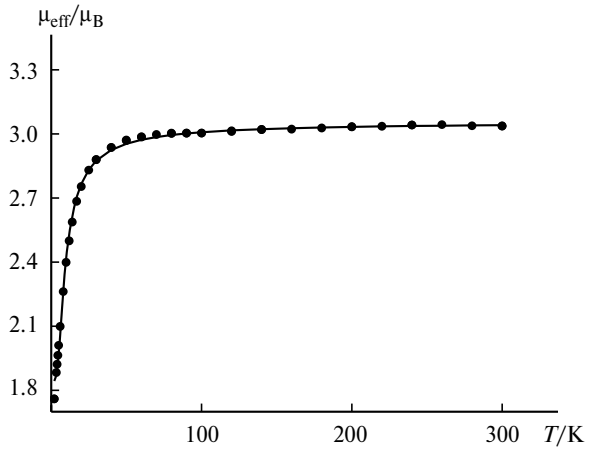

Fig. 4. Temperature dependence of the effective magnetic moment (μ_{eff}) for $[Cu(hfac)_2(L^{5Et})_2]$). The solid line represents the theoretical curve.

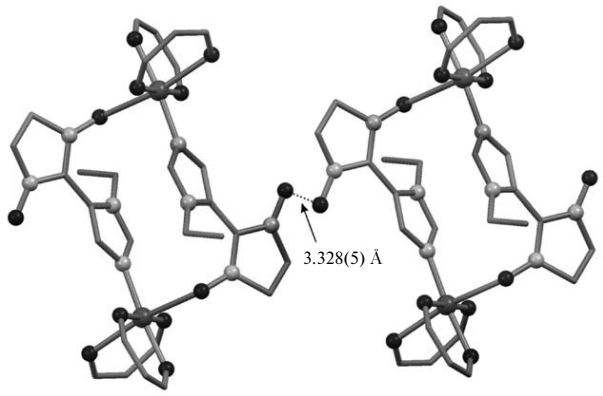

Fig. 5. Molecular structure of $[Cu(hfac)_2L^{5Et}]_2$ and the shortest contact between the molecules ($T = 296$ K).

(296, 240, 95, and 30 K). It can be seen that these values change little when decreasing the temperature, and their dynamics practically reflects the natural crystal compression process caused by cooling. We note that in this case, the exact bond lengths and bond angles in the compound molecule with varying temperature are not as important, while the fact of the insignificant change in the $[Cu(hfac)_2L^{5Et}]_2$ structural characteristics when varying the experimental temperature in a wide range is of great importance. This is caused by the following factors.

It is known that heterospin Cu^{2+} complexes with nitroxide radicals can undergo heat- and light-induced structural rearrangements[8—14] accompanied by considerable changes in the distances between paramagnetic centers in the metal atom coordination sphere. Such structural rearrangements lead to a change in the energy and/or sign of exchange interactions and appear as anomalies in the

Table 2. Temperature dependence of some bond lengths and bond angles in the $[Cu(hfac)_2L^{5Et}]_2$ molecule

Parameter	$[Cu(hfac)_2L^{5Et}]_2$			
	296 K	240 K	95 K	30 K
Bond/Å				
Cu—O_{NO}	2.476(4)	2.4356(18)	2.3952(15)	2.414(11)
Cu—N	1.971(4)	1.9846(18)	1.9785(16)	1.993(12)
Cu—O_{hfac}	2.302(4)	2.2998(19)	2.3002(15)	2.318(11)
	1.961(4)	1.9570(16)	1.9595(14)	1.974(10)
	1.963(4)	1.9655(16)	1.9631(14)	1.971(10)
	1.943(3)	1.9686(17)	1.9686(14)	1.987(10)
N—O	1.278(5)	1.287(2)	1.289(2)	1.295(16)
	1.268(5)	1.268(3)	1.272(2)	1.280(16)
—O...O—	3.328(5)	3.313(3)	3.282(2)	3.31(2)
Angle/deg				
CuON	131.4(3)	128.08(15)	125.83(11)	126.9(9)
(Et—N)—Im	75.1	71.8	71.5	71.8
(CN_2O_2)—Im	38.3	37.5	37.7	38.0

$\mu_{eff}(T)$ curves. These anomalies can be quite diverse: they can be observed at different temperatures and in different temperature ranges, be accompanied by hysteresis, be step-like, be either sharp or smooth. Therefore, it is difficult to determine the cause of the emergence of anomalies only from the form of the $\mu_{eff}(T)$ dependence. Moreover, anomalies in the $\mu_{eff}(T)$ curve for multispin compounds can also appear as a consequence of the existence of exchange clusters with exchange of a different sign, *i.e.*, in the absence of any noticeable phase structural rearrangements in response to external stimuli.[15,16]

The $\mu_{eff}(T)$ dependence for $[Cu(hfac)_2L^{5Et}]_2$ also shows an anomaly (Fig. 6). At 300 K, the μ_{eff} value is equal to 3.45 μ_B. It is in good agreement with the spin-only value 3.46 μ_B for four noninteracting paramagnetic centers (two Cu^{2+} ions and two nitroxide radicals) and changes little when decreasing the temperature to 120 K. Upon further cooling, the μ_{eff} value rapidly decreases and tends to reach a plateau in the region of ~2.5 μ_B, which corresponds to two noninteracting paramagnetic centers with spins $S = 1/2$. Such a jump in the $\mu_{eff}(T)$ curve for $[Cu(hfac)_2L^{5Et}]_2$ can be related to the disappearance of one half of the spins in the four-center exchange clusters based on binuclear molecules, the structure of which is similar to that of $[Cu(hfac)_2L^{5Et}]_2$, a phenomenon previously described for "breathing" crystals.[17–19] However, the X-ray diffraction data for $[Cu(hfac)_2L^{5Et}]_2$, given above, which were taken in a wide temperature interval, demonstrate that this complex cannot be regarded as a "breathing" crystal. Thus, the difficulty of choosing the correct theoretical model for describing the experimental $\mu_{eff}(T)$ dependence for $[Cu(hfac)_2L^{5Et}]_2$ prompted us to study the solid phase of the complex by ESR.

At 300 K, the spectrum of the $[Cu(hfac)_2L^{5Et}]_2$ powder is a poorly-resolved exchange-narrowed line. However, when cooling the sample from 300 K to 5 K, this spectrum

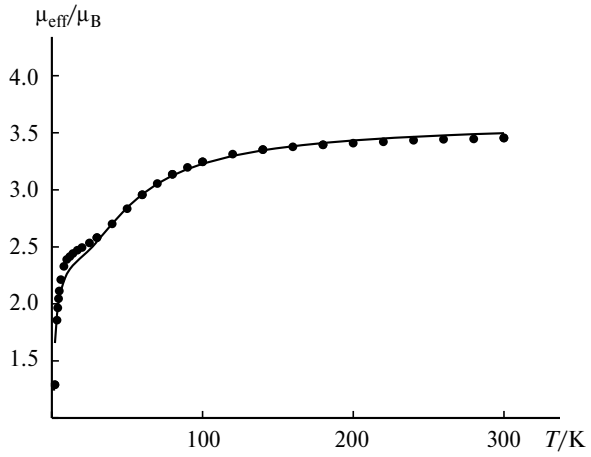

Fig. 6. Temperature dependence of the effective magnetic moment (μ_{eff}) for $[Cu(hfac)_2L^{5Et}]_2$. The solid line represents the theoretical curve.

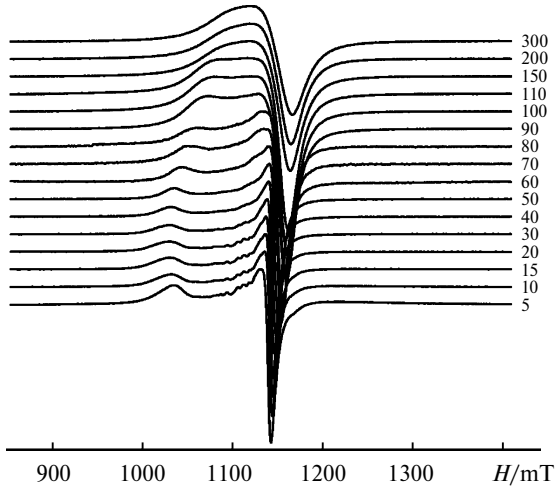

Fig. 7. Temperature dependence of Q-band ESR spectra ($\nu_{mw} \approx$ $\approx$ 34.18 GHz) of a $[Cu(hfac)_2L^{5Et}]_2$ powder sample. The temperature values are indicated in the Figure.

is gradually transformed into the characteristic ESR spectrum of the Cu^{2+} ion in the axially-symmetric octahedral environment (Fig. 7). The spectrum in question is characterized by an anisotropic g-tensor with $g_\parallel > g_\perp$. Meanwhile, the typical splitting due to hyperfine interaction (HFI) with a copper nuclear spin ($I = 3/2$) on the longitudinal component ($g_\parallel$) is not observed. From this we conclude that the exchange narrowing is also realized at helium temperatures. The nitroxide radical spins do not contribute to the observed spectra either as a component of the exchange-coupled system or as separate signals of magnetically isolated centers. Thus, based on the temperature transformation of $[Cu(hfac)_2L^{5Et}]_2$ powder ESR spectra, it can be unequivocally concluded that when decreasing the temperature, the spins of nitroxide radicals disappear, *i.e.*, they pair up with each other.

The ESR spectrum at 10 K can be adequately simulated using typical parameters of the Cu^{2+} ion in an octahedral environment with axial symmetry ($g_\parallel \approx 2.3, g_\perp \approx 2.071$), except the averaging of the HFI on the longitudinal component of the experimental spectrum (Fig. 8, *a*). The numerical solution of the modified Bloch equations was used to calculate the full temperature dependence of the ESR spectra. Taking into account the specific features of the spin density distribution in such ligands (its predominant localization on the N—O—C—O—N fragment of the nitronyl nitroxide radical)[7] and the presence, according to X-ray diffraction data for $[Cu(hfac)_2L^{5Et}]_2$ (see Fig. 5), of potentially efficient intermolecular contacts between neighboring molecules,[7,20] we considered a structural fragment consisting of four paramagnetic centers {Cu^{2+}—O←N—C=N—•O···O•—N—C=N→O—Cu^{2+}}, in which each Cu^{2+}—O•—N pair belongs to neighboring cyclic molecules.

In the model in question, the highest energy exchange interaction between radicals has an intermolecular nature.

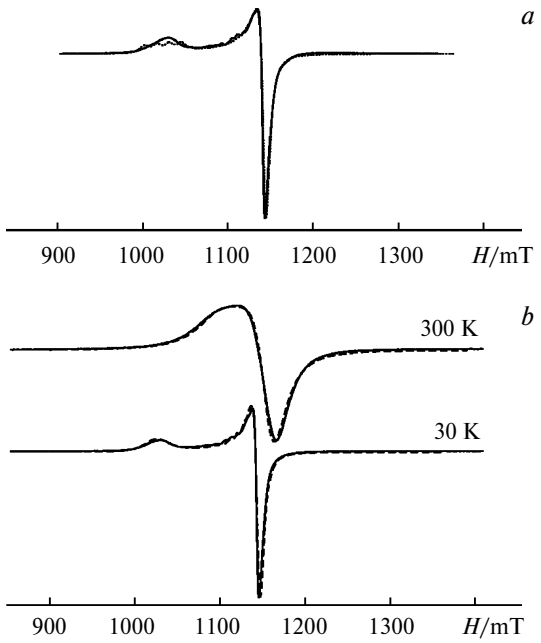

Fig. 8. (*a*) Experimental (solid line) and calculated (dashed line) ESR spectra of $[Cu(hfac)_2L^{5Et}]_2$ at 10 K. The calculated spectrum was obtained for a model of the powder spectrum of a single Cu^{2+} ion with parameters $g_\parallel = 2.3$, $g_\perp = 2.071$, $A_\parallel = 450$ MHz. (*b*) Experimental (solid line) and calculated (dashed line) ESR spectra of $[Cu(hfac)_2L^{5Et}]_2$ at 300 and 30 K. The temperature values are indicated in the Figure. The calculated spectra were obtained by numerical solution of the modified Bloch equations with parameters $g_\parallel = 2.3$, $g_\perp = 2.071$, $A_\parallel = 450$ MHz for the Cu^{2+} ion; $g = 2.007$ for the radical; $T_{2,Cu} = 1.7$ ns, $T_{2,NO} = 1.7$ ns, and $J = 0.3$ K at 300 K; $T_{2,Cu} = 6$ ns, $T_{2,NO} = 6$ ns, and $J = 0.03$ K at 30 K; $\alpha = 1$ at 300 K and $\alpha = 0$ at 30 K.

Since two spins of identical radicals pair up when the temperature decreases, in order to simplify the calculations, it is sufficient to consider the Cu^{2+}—N—•O dimer with the exchange interaction $J_{Cu\text{-}NO}$ and a temperature-dependent contribution of the radical fraction $\alpha(T)$ to the total magnetization of the sample ($0 < \alpha < 1$, $\alpha(5\text{ K}) = 0$ corresponds to zero contribution of nitroxides to the spectrum). Due to the presence of HFI with $I = 3/2$, the IR spectrum of the Cu^{2+} ion in an arbitrary orientation is composed of four lines. The HFI constants of nitroxide radicals can be neglected due to their insignificance compared to the HFI of the Cu^{2+} ion, and the nitroxide spectrum can be considered as being composed of one singlet line. Thus, the system of modified Bloch equations should be written in the following form

$$\begin{cases} \dfrac{dG^{NO}}{dt} = \left(-\dfrac{1}{T_2^{NO}} - i\left(\varpi - \varpi^{NO}\right) - \dfrac{1}{\tau^{NO}}\right)G^{NO} + \sum\limits_{i=1-4}\dfrac{G^{Cu,i}}{\tau^{Cu,i}} - i\varpi_1 M_0^{NO} \\ \dfrac{dG^{Cu,i}}{dt} = \left(-\dfrac{1}{T_2^{Cu,i}} - i\left(\varpi - \varpi^{Cu,i}\right) - \dfrac{1}{\tau^{Cu,i}}\right)G^{Cu,i} + \dfrac{G^{NO}}{\tau^{NO}} - i\varpi_1 M_0^{Cu,i} \end{cases}, \quad (1)$$

where the second equation of the system is written for the four Cu^{II} lines (i = 1—4). The variables $G^{NO,Cu,i} = M_x^{NO,Cu,i} - iM_y^{NO,Cu,i}$ characterize the longitudinal magnetization of each center, $M_0^{NO,Cu,i}$ characterizes the corresponding equilibrium magnetization, ω^i characterizes the corresponding resonance frequencies, ω_1 is the amplitude of the detecting microwave field, $T_2^{NO,Cu,i}$ are the longitudinal relaxation times. The $\tau^{NO,Cu,i}$ values describe the electron lifetime on each paramagnetic center in the process of its migration between them, while their ratio characterizes the portion of the corresponding spins in the exchange-coupled system, *i.e.*, $\tau^{NO}/\tau^{Cu,i} \equiv \alpha$. The order of magnitude of time can, as a rule, be estimated as $\tau \sim 1/2J$, where J is the exchange interaction in the system of centers corresponding to a spin Hamiltonian of the form $-2J \cdot S^i S^j$ (in our case, $J = J_{Cu-ON}$; J_{NO-ON} is included through the temperature-dependent coefficient $\alpha(T)$).

To solve the system of equations (1), first we calculated the resonance frequencies ω^j for each orientation of the dimer Cu^{2+}—O•—N relative to the magnetic field, then we found the stationary solution of the system of equations (1) ($dG^{NO,Cu,i}/dt = 0$), and the ESR spectrum was calculated as $I = -\mathrm{Im}(G^{NO} + \sum\limits_{i=1-4} G^{Cu,i})$. Finally, we found the sum of all orientations to obtain the final powder ESR spectrum. Note that we have successfully used this approach earlier to describe the exchange processes in Cu^{2+} clusters with nitroxide radicals.[21—24]

Figure 8, *b* shows a good agreement between the experimental and calculated ESR spectra both at 300 K ($\alpha = 1$) and 30 K ($\alpha = 0$), which confirms the qualitative conclusions about the presence of nitroxide radical spins at high temperatures and their full pairing up at $T < 50$ K. The characteristic temperature of the complete disappearance of nitroxide spins is well correlated with the completion of the principal decrease in the magnetic moment at $T \sim 40$—50 K.

According to the results of ESR, the $\mu_{eff}(T)$ dependence for $[Cu(hfac)_2L^{5Et}]_2$ was analyzed using a tetramer model ($H = -2J_1(S_{Cu1}S_{R1} + S_{R2}S_{Cu2}) - 2J_2 \cdot S_{R1}S_{R2}$), the intermolecular exchange interactions were taken into account in the molecular field approximation. As a result, the following optimal values of the J_1, J_2, zJ' parameters and g-factor were obtained: 0.8, −39, −1.8, and 2.09 cm^{-1}, respectively.

In conclusion, in this study we successfully synthesized a heterospin complex $[Cu(hfac)_2(L^{5Et})_2]$ which has a packing similar to that of the jumping $[Cu(hfac)_2(L^{5Me})_2]$ crystals studied earlier. It was found that the lengthening of intermolecular O···O contacts between neighboring nitroxide groups in $[Cu(hfac)_2(L^{5Et})_2]$ as compared to those in $[Cu(hfac)_2(L^{5Me})_2]$ by 0.3—0.5 Å quenches chemomechanical motion. It was confirmed that when cooling binuclear $[Cu(hfac)_2L^{5Et}]_2$ crystals the antiferromagnetic exchange between the unpaired electrons of the >N—•O groups of neighboring molecules leads to a full spin-paring in nitroxides at 40—50 K. At low temperatures, only Cu^{2+} ions contribute to the paramagnetism of the compound.

Experimental

2,3-Bis(hydroxyamino)-2,3-dimethylbutane[25] and 2-(1*H*-imidazol-4-yl)-4,4,5,5-tetramethyl-4,5-dihydro-1*H*-imidazole 3-oxide-1-oxyl[26] were synthesized according to known procedures. Commercial reagents and solvents were used as received. TLC was performed on Aluminium oxide N/UV_{254} plates with a pre-coated sorbent layer on a polymeric substrate. For column chromatography silica gel (0.063—0.200 mm, Merck) was used. Elemental analysis was performed on an Euro EA 3000 microanalyzer in the Chemical Multi-access Service Center of the Siberian Branch of the Russian Academy of Sciences. IR spectra were recorded on a Bruker Vector-22 spectrophotometer in KBr pellets.

2-(1-Ethylimidazol-4-yl)-4,4,5,5-tetramethyl-4,5-dihydro-1*H*-imidazole 3-oxide-1-oxyl (L^{4Et}) and 2-(1-ethylimidazol-5-yl)-4,4,5,5-tetramethyl-4,5-dihydro-1*H*-imidazole 3-oxide-1-oxyl (L^{5Et}). Diethyl sulfate (2.4 g, 0.016 mol) was added to a suspension of imidazole-4-carbaldehyde (1.5 g, 0.016 mol) in anhydrous acetone (15 mL). The reaction mixture was refluxed for 18 h with stirring without contact with air moisture. Then the mixture was neutralized with an excess of moist $NaHCO_3$ and the precipitate that formed was filtered and washed with EtOH. The filtrate was dried with Na_2SO_4 and concentrated using a rotary evaporator. The residue was filtered through a layer of Al_2O_3 (1.5×10 cm), the eluent was AcOEt. The filtrate was concentrated *in vacuo* and a light yellow oil (1.0 g) was obtained, which contained a mixture of isomers of 1-ethyl-1*H*-imidazole-4-carbaldehyde and 1-ethyl-1*H*-imidazole-5-carbaldehyde. Then the obtained mixture along with 2,3-bis(hydroxyamino)-2,3-dimethylbutane (1.2 g, 0.008 mol) was dissolved in MeOH (10 mL). The solution was stirred for 12 h at 20 °C and concentrated. AcOEt was added to the oil-like residue, the precipitate that formed was filtered and washed with AcOEt. The obtained precipitate (0.752 g) was dissolved in EtOH (15 mL), MnO_2 (3.7 g) was added to the solution, and the mixture was stirred for 4 h at ~20 °C, then filtered and concentrated. The residue was subjected to chromatography on a column with SiO_2 (1.5×50 cm), the eluent was AcOEt—MeOH (10 : 1). The first fraction contained nitroxide L^{5Et}, the second contained its isomer, L^{4Et}. Both fractions were concentrated, the obtained products were crystallized from a mixture of CH_2Cl_2 with heptane. The yield of L^{5Et} was 0.342 g (8.5% calculated on 1*H*-imidazole-4-carbaldehyde), dark blue crystals, m.p. 141—142 °C (from a mixture of CH_2Cl_2—*n*-heptane), R_f 0.83 (AcOEt—MeOH, 3 : 2) on the Aluminium oxide N/UV_{254} plates. IR, ν/cm^{-1}: 3415, 3096, 2990, 2933, 1715, 1676, 1583, 1493, 1456, 1421, 1399, 1386, 1364, 1351, 1327, 1250, 1231, 1216, 1166, 1140, 1122, 1050, 960, 925, 871, 840, 805, 754, 661, 608, 539. Found (%): C, 57.1; H, 7.4; N, 22.4. $C_{12}H_{19}N_4O_2$. Calculated (%): C, 57.4; H, 7.6; N, 22.3.

The yield of L^{4Et} was 0.223 g (5.6% calculated on 1*H*-imidazole-4-carbaldehyde), dark blue crystals, m.p. 121—122 °C, R_f 0.70 (AcOEt—MeOH, 3 : 2) on the Aluminium oxide N/UV_{254} plates. IR, ν/cm^{-1}: 3422, 3184, 3114, 2982, 2936, 1632, 1580, 1510, 1450, 1396, 1366, 1338, 1286, 1259, 1232, 1213, 1167, 1131, 1110, 1052, 1012, 987, 964, 867, 816, 786, 755, 665, 633, 542. Found (%): C, 57.3; H, 7.6; N, 22.6. $C_{12}H_{19}N_4O_2$. Calculated (%): C, 57.4; H, 7.6; N, 22.3.

Table 3. Crystallographic characteristics, X-ray data collection, and structure refinement statistics for L^{4Et}, L^{5Et}, $[Cu(hfac)_2(L^{5Et})_2]$, and $[Cu(hfac)_2L^{5Et}]_2$

Parameter	L^{4Et}	L^{5Et}	$[Cu(hfac)_2(L^{5Et})_2]$		$[Cu(hfac)_2L^{5Et}]_2$		
Formula	$C_{12}H_{19}N_4O_2$	$C_{12}H_{19}N_4O_2$	$C_{34}H_{40}CuF_{12}N_8O_8$		$C_{44}H_{42}Cu_2F_{24}N_8O_{12}$		
M	251.31	251.31	980.28		1457.94		
T/K	296	296	296	296	240	95	30
Space group	$P2_1/c$	$P2_1/n$	P-1	$P2_1/c$	$P2_1/c$	$P2_1/c$	$P2_1/c$
Z	4	4	1	2	2	2	2
a/Å	10.488(2)	7.7145(3)	7.389(2)	10.417(2)	10.2518(3)	10.1486(11)	10.280(4)
b/Å	11.371(2)	14.7488(6)	11.761(3)	15.598(3)	15.4780(5)	15.2713(17)	15.352(5)
c/Å	12.058(2)	11.8269(4)	14.222(3)	21.607(5)	21.2067(7)	20.959(2)	21.106(6)
α/deg				111.829(19)			
β/deg	111.923(11)	103.067(2)	98.07(2)	101.509(11)	100.9642(17)	100.499(5)	79.71
γ/deg				98.59(2)			
V/Å^3	1334.0(5)	1310.82(9)	1108.2(5)	3440.2(12)	3303.60(18)	3193.9(6)	3277.4(19)
d_{calc}/g cm^{-3}	1.251	1.273	1.469	1.407	1.466	1.516	1.477
θ/deg	28.138	28.00	28.094	28.469	67.434	66.206	28.825
Number of measured/independent reflections	11455/3198	11980/3149	15617/5283	53778/8436	24180/5770	48281/5540	14340/7540
R_{int}	0.0307	0.0337	0.1156	0.1662	0.0264	0.0242	0.5898
I_{hkl} ($I > 2\sigma(I)$)	2067	1949	1938	2655	4812	5047	2287
N	169	169	288	488	514	487	406
GOOF	1.146	1.101	0.971	0.867	1.064	1.092	1.074
R_1	0.0481	0.0456	0.0950	0.0722	0.0397	0.0355	0.1613
wR_2 ($I > 2\sigma(I)$)	0.1313	0.1155	0.2893	0.1749	0.1097	0.0951	0.3909
R_1	0.0826	0.0826	0.2141	0.2385	0.0500	0.0396	0.3564
wR_2 (all data)	0.1485	0.1331	0.3338	0.2251	0.1204	0.0996	0.4649
CCDC	1486108	1486105	1486106	1486110	1486111	1486109	1486107

2-(1-Ethylimidazol-4-yl)-4,4,5,5-tetramethyl-4,5-dihydro-1*H*-imidazole 3-oxide-1-oxyl (L^{4Et}). A mixture of 4,4,5,5-tetramethyl-2-(1*H*-imidazol-4-yl)-4,5-dihydro-1*H*-imidazole 3-oxide-1-oxyl (0.223 g, 1.0 mmol), Bu^{t}OK (0.115 g, 1.02 mmol), and DMF (5 mL) was stirred for 20 min under Ar. Diethyl sulfate (0.154 g, 1.0 mmol) was added to the reaction mixture, after which it was stirred for 3 h at ~20 °C, then concentrated *in vacuo*. The product was purified using column chromatography to obtain nitroxide L^{4Et} (0.186 g, 83%).

Bis(1,1,1,5,5,5-hexafluoropentane-2,4-dionato)bis[2-(1-ethylimidazol-5-yl)-4,4,5,5-tetramethyl-4,5-dihydro-1*H*-imidazole 3-oxide-1-oxyl]copper(II) [Cu(hfac)$_2$ (L^{5Et})$_2$]. A solution of Cu(hfac)$_2$ (0.076 g, 0.16 mmol) and L^{5Et} (0.04 g, 0.32 mmol) in acetone (2 mL) was diluted with EtOH (3 mL) and allowed to stand for 48 h at −18 °C. The precipitated blue crystals were collected by filtration and dried in air. The yield was 0.045 g (85%). Found (%): C, 42.3; H, 4.4; N, 11.1; F 22.4. $C_{34}H_{40}CuF_{12}N_8O_8$. Calculated (%): C, 41.7; H, 4.1; N, 11.4; F, 23.3.

Bis{bis(1,1,1,5,5,5-hexafluoropentane-2,4-dionato)[2-(1-ethylimidazol-5-yl)-4,4,5,5-tetramethyl-4,5-dihydro-1*H*-imidazole 3-oxide-1-oxyl]copper(II)} [Cu(hfac)$_2$L^{5Et}]$_2$. A solution of Cu(hfac)$_2$ (0.076 g, 0.16 mmol) and L^{5Et} (0.04 g, 0.16 mmol) in anhydrous CH_2Cl_2 (2 mL) was diluted with hexane (4 mL) and allowed to stand for 48 h at −18 °C without contact with air moisture. The crystals formed as cubic aggregates were collected by filtration and washed with ice-cold hexane. The yield was 0.098 g (80%). Found (%): C, 36.8; H, 3.1; N, 7.5; F, 29.5. $C_{44}H_{42}Cu_2F_{24}N_8O_{12}$. Calculated (%): C, 36.3; H, 2.9; N, 7.7; F, 31.3.

X-ray diffraction. X-ray diffraction data set from single crystals were collected on SMART APEX II and SMART APEX DUO diffractometers (Bruker AXS) (Mo-$K\alpha$, λ = 0.71073 Å, correction for absorption was applied using the Bruker SADABS program, version 2.10). The structures were solved using direct methods, refined using the full-matrix least squares method with anisotropic displacement parameters for all nonhydrogen atoms. Positions of H atoms were calculated geometrically and refined using a riding model. The structure solution and refinement were carried out using the Shelxs-97 and the Shelxl-2014/6 program package. Table 3 gives the crystallographic characteristics, details of X-ray diffraction experiments, and the numbers of the structures deposited in the Cambridge Crystallographic Data Center. The complete data for the structures can be obtained as cif-files upon request at http://www.ccdc.cam.ac.uk/data_request/cif.

Magnetic susceptibility (χ) of the polycrystalline samples was measured on a Quantum Design MPMSXL SQUID magnetometer in a temperature range of 2—300 K with a magnetic field equal to 5 kOe. The paramagnetic contributions of magnetic susceptibility were determined taking into account the diamagnetic contribution estimated using Pascal´s constants. The effective magnetic moment was calculated by the following formula

$$\mu_{eff} = [3k\chi T/(N_A\mu_B^2)]^{1/2},$$

where N_A is Avogadro´s number, μ_B is the Bohr magneton, k is the Boltzmann constant.

The Q-band ESR spectra (34 GHz) were obtained on a commercial Bruker Elexsys E580 spectrometer equipped with a cryostat and temperature unit, in the continuous wave mode. In all the ESR experiments, the samples were studied in the form of powder placed into quartz ampules. Simulation was carried out using the EasySpin software.[27]

The work was financially supported by the Russian Science Foundation (Project No. 15-13-30012), Federal Agency for Scientific Organizations (Project No. 0333-2015-0004), Russian Foundation for Basic Research (Project No. 15-53-10009), the Council on Grants at the President of the Russian Federation (Program for State Support of Young Scientists, Grants MK-6040.2016.3 and MK-8345.2016.3). ESR experiments were financially supported by the Russian Foundation for Basic Research (Project Nos 14-03-00224 and 15-03-07640) and Federal Agency for Scientific Organizations (Project No. 0333-2014-0001).

References

1. V. I. Ovcharenko, S. V. Fokin, E. Yu. Fursova, O. V. Kuznetsova, E. V. Tretyakov, G. V. Romanenko, A. S. Bogomyakov, *Inorg. Chem.*, 2011, **50**, 4307.
2. V. I. Ovcharenko, E. V. Tretyakov, S. V. Fokin, E. Yu. Fursova, O. V. Kuznetsova, S. E. Tolstikov, G. V. Romanenko, A. S. Bogomyakov, R. Z. Sagdeev, *Russ. Chem. Bull.* (*Int. Ed.*), 2011, **60**, 2457 [*Izv. Akad. Nauk*, *Ser. Khim.*, 2011, 2411].
3. E. V. Tretyakov, S. V. Fokin, E. Yu. Fursova, O. V. Kuznetsova, G. V. Romanenko, R. Z. Sagdeev, V. I. Ovcharenko, *Russ. Chem. Bull.* (*Int. Ed.*), 2013, **62**, 1803 [*Izv. Akad. Nauk*, *Ser. Khim.*, 2013, 1803].
4. V. Ovcharenko, E. Fursova, G. Romanenko, I. Eremenko, E. Tretyakov, V. Ikorskii, *Inorg. Chem.*, 2006, **45**, 5338.
5. E. V. Tretyakov, V. I. Ovcharenko, *Russ. Chem. Rev.*, 2009, **78**, 1051.
6. S. Vancoillie, L. Rulíšek, F. Neese, K. Pierloot, *J. Phys. Chem. A*, 2009, **113**, 6149.
7. M. V. Fedin, S. L. Veber, K. Yu. Maryunina, G. V. Romanenko, E. A. Suturina, N. P. Gritsan, R. Z. Sagdeev, V. I. Ovcharenko, E. G. Bagryanskaya, *J. Am. Chem. Soc.*, 2010, **132**, 13886.
8. P. Rey, V. I. Ovcharenko, in *Magnetism: Molecules to Materials*, *IV*, Eds J. S. Miller, M. Drillon, Wiley-VCH, New York, 2003, p. 41.
9. V. I. Ovcharenko, K. Yu. Maryunina, S. V. Fokin, E. V. Tretyakov, G. V. Romanenko, V. N. Ikorskii, *Russ. Chem. Bull.* (*Int. Ed.*), 2004, **53**, 2406 [*Izv. Akad. Nauk*, *Ser. Khim.*, 2004, 2304].
10. V. I. Ovcharenko, G. V. Romanenko, K. Yu. Maryunina, A. S. Bogomyakov, E. V. Gorelik, *Inorg. Chem.*, 2008, **47**, 9537.
11. V. I. Ovcharenko, E. G. Bagryanskaya, in *Spin-Crossover Materials: Properties and Applications*, Ed. M. A. Halcrow, John Wiley&Sons, UK, 2013, p. 239.
12. M. Fedin, V. Ovcharenko, R. Sagdeev, E Reijerse, W. Lubitz, E. Bagryanskaya, *Angew. Chem. Int. Ed.*, 2008, **47**, 6897.
13. M. V. Fedin, K. Yu. Maryunina, R. Z. Sagdeev, V. I. Ovcharenko, E. G. Bagryanskaya, *Inorg. Chem.*, 2012, **51**, 709.
14. W. Kaszub, A. Marino, M. Lorenc, E. Collet, E. G. Bagryanskaya, E. V. Tretyakov, V. I. Ovcharenko, M. V. Fedin, *Angew. Chem. Int. Ed.*, 2014, **53**, 10636.
15. V. Gorelik, V. I. Ovcharenko, M. Baumgarten, *Eur. J. Inorg. Chem.*, 2008, 2837.
16. K. Yu. Maryunina, G. V. Romanenko, E. M. Zueva, S. V. Fokin, A. S. Bogomyakov, V. I. Ovcharenko, *Russ. Chem.*

Bull. (*Int. Ed.*), 2013, **62**, 2337 [*Izv. Akad. Nauk*, *Ser. Khim.*, 2013, 2337].
17. F. Lanfranc de Panthou, E. Belorizky, R. Calemczuk, D. Luneau, C. Marcenat, E. Ressouche, P. Turek, P. Rey, *J. Am. Chem. Soc.*, 1995, **117**, 11247.
18. N. A. Artiukhova, K. Yu. Maryunina, S. V. Fokin, E. V. Tretyakov, G. V. Romanenko, A. V. Polushkin, A. S. Bogomyakov, R. Z. Sagdeev, V. I. Ovcharenko, *Russ. Chem. Bull.* (*Int. Ed.*), 2013, **62**, 2132 [*Izv. Akad. Nauk*, *Ser. Khim.*, 2013, 2132].
19. S. E. Tolstikov, N. A. Artiukhova, G. V. Romanenko, A. S. Bogomyakov, E. M. Zueva, I. Yu. Barskaya, M. V. Fedin, K. Yu. Maryunina, E. V. Tretyakov, R. Z. Sagdeev, V. I. Ovcharenko, *Polyhedron*, 2015, **100**, 132.
20. S. L. Veber, M. V. Fedin, K. Yu. Maryunina, G. V. Romanenko, R. Z. Sagdeev, E. G. Bagryanskaya, V. I. Ovcharenko, *Inorg. Chim. Acta*, 2008, **361**, 4148.
21. M. V. Fedin, S. L. Veber, I. A.Gromov, V. I. Ovcharenko, R. Z. Sagdeev, E. G. Bagryanskaya, *Phys. Chem. A*, 2007, **111**, 4449.
22. M. V. Fedin, I. Yu. Drozdyuk, E. V. Tretyakov, S. E. Tolstikov, V. I. Ovcharenko, E. G. Bagryanskaya, *Appl. Magn. Reson.*, 2011, **41**, 383.
23. M. V. Fedin, S. L. Veber, E. G. Bagryanskaya, G. V. Romanenko, V. I. Ovcharenko, *Dalton Trans.*, 2015, **44**, 18823.
24. M. V. Fedin, S. L. Veber, E. G. Bagryanskaya, V. I. Ovcharenko, *Coord. Chem. Rev.*, 2015, **289—290**, 341—356.
25. V. I. Ovcharenko, S. V. Fokin, G. V. Romanenko, I. V. Korobkov, P. Rey, *Russ. Chem. Bull.* (*Engl. Transl.*), 1999, **48**, 1519 [*Izv. Akad. Nauk*, *Ser. Khim.*, 1999, 1539].
26. E. Yu. Fursova, V. I. Ovcharenko, G. V. Romanenko, E. V. Tretyakov, *Tetrahedron Lett.*, 2003, **44**, 6397.
27. S. Stoll, A. Schweiger, *J. Magn. Reson.*, 2006, **178**, 42.

Received June 17, 2016;
in revised form September 28, 2016